Designing binuclear transition metal complexes: a new example of the versatility of *N*,*N*′-bis(2-aminobenzyl)-4,13-diaza-18-crown-6

Lea Vaiana[a], Carlos Platas-Iglesias[a], David Esteban-Gómez[a], Fernando Avecilla[a], Juan Modesto Clemente-Juan[b], José Antonio Real[b], Andrés de Blas[a] and Teresa Rodríguez-Blas[a]

[a] Departamento de Química Fundamental, Universidade da Coruña, Campus da Zapateira s/n, 15071 A Coruña, Spain

[b] Institut de Ciencia Molecular/Departament de Química Inorgánica, Universitat de València, Doctor Moliner 50, Burjassot, Spain

Dalton Transactions Issue 11, pages 2031–2037, 07 June 2005
Received 02 March 2005, Accepted 13 April 2005, First published 27 April 2005

How to cite:

Designing binuclear transition metal complexes: a new example of the versatility of *N*,*N*′-bis(2-aminobenzyl)-4,13-diaza-18-crown-6. L. Vaiana, C. Platas-Iglesias, D. Esteban-Gómez, F. Avecilla, J. M. Clemente-Juan, J. A. Real, A. de Blas and T. Rodríguez-Blas, *Dalt. Trans.*, 2005, 2031–2037. DOI: 10.1039/B503151F.

Abstract

N,*N*′-Bis(2-aminobenzyl)-4,13-diaza-18-crown-6 (L) is a versatile receptor able to adapt to the coordinative preferences of different metal cation guests. With first-row transition metal ions, L tends to form binuclear complexes but, depending on the nature of the particular metal ion, the structure of the binuclear complex may be very different. Herein we report a study of the structure and magnetic properties of the corresponding nickel(II) and cobalt(II) complexes. The X-ray crystal structure of the nickel complex (**1**), with formula $[Ni_2(L)(CH_3CN)_4](ClO_4)_4 \cdot CH_3CN$, shows that this compound presents a symmetric coordination environment with L adopting an *anti* arrangement. Each Ni(II) ion is six-coordinate in a distorted octahedral environment, and both metal ions are quite far from each other. On the other hand, the X-ray crystal structure of the cobalt complex (**2**), with formula $[Co(L)(\mu\text{-}OH)Co(CH_3CN)](ClO_4)_3$, reveals a rather different structure. Coordination number asymmetry is found: one of the Co(II) is five-coordinate in a distorted trigonal-bipyramidal coordination environment, while the second Co(II) ion is six-coordinate in a distorted octahedral arrangement. Now L adopts a *syn* arrangement and a hydroxide group acts as a bridge between both cobalt ions. This hydroxo-bridged Co(II) binuclear complex shows structural features that mimic the active site of methionine aminopeptidases. The magnetic properties of **1** and **2** have been investigated in the temperature range 2.0–300 K. Whereas **1** displays a Curie law except for temperatures below 50 K where zero-field splitting of the $S = 1$ ground state is observed, antiferromagnetic exchange in the singular asymmetric binuclear Co(II) complex **2** has been observed. This magnetic behaviour has been fitted considering first-order spin–orbit coupling in the assumed axially distorted octahedral site and totally quenched orbital contribution in the five-coordinate site in which zero-field splitting of the $S = 3/2$ ground state is operative.

Keywords: macrocyclic ligands; crystal structures; binuclear complexes; crown ethers; transition-metal complexes

Introduction

Bi- and oligonuclear complexes containing transition metals are of considerable interest for designing new magnetic materials with potential use in information storage,[1,2] for the stabilization of unusual oxidations states,[3] or for investigating the relationship between the structure and the role of the polymetallic active sites in biological systems.[4] Indeed, biochemistry of both nickel and cobalt is now well documented.[5,6] In particular, metallohydrolases are an important group of binuclear metalloenzymes that catalyse the hydrolysis of a range of peptide and phosphate ester bonds.[7] A binuclear Ni(II) core is present in urease,[8] while the active site of methionine aminopeptidase[9] contains a binuclear Co(II) core.

Bimetallic complexes are very often formed by bridging ligands that can mediate magnetic interactions between paramagnetic metal ions. The mechanism of the interaction between two magnetic 3d ions within a binuclear species is nowadays rather well understood.[10] Although the factors governing the nature (antiferro- or ferromagnetic), and the magnitude of this interaction to some extent can be controlled, and it is now possible to design magnetic systems with predictable properties, some situations remain uncertain. For instance, the theoretical treatment of binuclear Co(II) complexes belongs to one of the more difficult chapters of magnetochemistry. The Co(II) d^7 ion is strongly anisotropic, and the first orbital momentum is no longer negligible so the isotropic exchange interaction is insufficient to discuss these complexes and must be supplemented by considerations of orbitally dependent exchange interactions.[11]

A large number of supporting ligands have been developed to favour the formation of polynuclear cores. Among the different strategies used to prepare bi- and polynuclear transition metal complexes are the use of symmetrical[12–14] or unsymmetrical[15] polydentate ligands, macrocyclic receptors,[16–18] or self-assembling processes.[19] Currently, we are interested in the chemistry of metal complexes supported by lariat crown ethers and related cryptands.[20–23] The bibracchial lariat ether *N*,*N'*-bis(2-aminobenzyl)-4,13-diaza-18-crown-6 (L, see Chart 1) is a versatile receptor able to adapt to the coordinative preferences of the metal cation guest. With Pb(II), as well as with alkaline earth and group 12 metals, L only forms mononuclear complexes, whereas with first-row transition metal ions, this receptor tends to form binuclear complexes.[24] Moreover, depending on the nature of the particular metal ion, the structure of the corresponding complex may be very different. Herein we discuss the structure of the corresponding nickel(II) and cobalt(II) binuclear complexes of formula $[Ni_2(L)(CH_3CN)_4](ClO_4)_4 \cdot CH_3CN$ **(1)** and $[Co(L)(\mu\text{-}OH)Co(CH_3CN)](ClO_4)_3$ **(2)**. The hydroxo-bridged Co(II) binuclear complex here presented shows structural features that mimic the active site of methionine aminopeptidases. Likewise, the magnetic properties of **1** and **2** have been investigated in the temperature range 2.0–300 K. The presence of a hydroxo bridging ligand in **2** allows magnetic interaction between the two Co(II) ions.

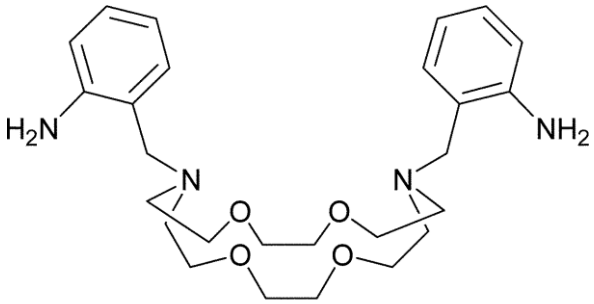

L

Chart 1

Experimental

Materials

All chemicals were purchased from commercial sources and used without further purification. Solvents were of reagent grade purified by the usual methods. *N*,*N*′-Bis(2-aminobenzyl)-4,13-diaza-18-crown-6 (L) was prepared as previously described.[24]

CAUTION! Perchlorate salts combined with organic ligands are potentially explosive and should be handled in small quantity and with the necessary precautions.[25]

Syntheses and characterization

$[Ni_2(L)(CH_3CN)_4](ClO_4)_4 \cdot CH_3CN$ (1). A mixture of *N*,*N*′-bis(2-aminobenzyl)-4,13-diaza-18-crown-6 (0.1017 g, 0.215 mmol) and $Ni(ClO_4)2 \cdot 6H_2O$ (0.1487 g, 0.423 mmol) in acetonitrile (25 cm^3) was stirred and heated to reflux over a period of 6 h. Slow diffusion of diethyl ether into the former solution at room temperature produced blue single-crystals suitable for X-ray diffraction that were collected by filtration and air-dried (yield: 0.1650 g, 65%) (Found: C, 35.69; H, 4.51; N, 10.63. $C_{36}H_{55}Ni_2Cl_4N_9O_{20}$ requires C, 36.24; H, 4.65; N, 10.57%). FAB mass spectrum: *m/z* (%BPI) 530 (15%) $[Ni(L)]^+$. ν_{max}/cm−1 (KBr): 3292, 3246 ($\nu(NH_2)$), 1618 ($\delta(NH_2)$), 1581 (ν(C=C)), 1088 (ν_{as}(Cl–O)), 627 (δ(O–Cl–O)) cm^{-1}. Λ_M (acetonitrile, $cm^2\ \Omega^{-1}\ mol^{-1}$): 455 (4 : 1 electrolyte).

$[Co(L)(\mu\text{-}OH)Co(CH_3CN)](ClO_4)_3$ (2). *N*,*N*′-Bis(2-aminobenzyl)-4,13-diaza-18-crown-6 (0.0970 g, 0.205 mmol) and $Co(ClO_4)_2 \cdot 6H_2O$ (0.1701 g, 0.465 mmol) were dissolved in acetonitrile (17 cm^3). The resultant pink solution was stirred and heated to reflux for 6 h and then allowed to cool to room temperature. Compound **2** was isolated as green crystals suitable for single-crystal X-ray diffraction analysis by slow diffusion of diethyl ether into the former solution (yield 0.0955 g, 49%) (Found: C, 35.80; H, 4.80; N, 7.48. $C_{28}H_{44}Cl_3Co_2N_5O_{17}$ requires C, 35.53; H, 4.67; N, 7.40%). FAB mass spectrum: *m/z* (%BPI) 805 (45%) $[Co_2(L)(\mu\text{-}OH)(ClO_4)_2]^+$, 787 (15%) $[Co_2(L)(ClO_4)_2]^+$, 707 (5%) $[Co_2(L)(\mu\text{-}OH)(ClO_4)]^+$, 687 (29%) $[Co_2(L)(ClO_4)]^+$. ν_{max}/cm^{-1} (KBr): 3392, 3305, 3261, 3128 ($\nu(NH_2)$), 1617 ($\delta(NH_2)$), 1587 (ν(C=C)), 1088 (ν_{as}(Cl–O)), 626 (δ(O–Cl–O)) cm^{-1}. Λ_M (acetonitrile, $cm^2\ \Omega^{-1}\ mol^{-1}$): 330 (3 : 1 electrolyte).

Physical measurements

Elemental analyses were carried out on a Carlo Erba 1108 elemental analyzer. FAB mass spectra were recorded using a FISONS QUATRO mass spectrometer with Cs ion-gun and 3-nitrobenzyl alcohol matrix. IR Spectra were recorded, as KBr discs, using a Bruker Vector 22 spectrophotometer. Conductivity measurements were carried out at 20ºC with a Crison Micro CM 2201 conductimeter using 10^{-3} M solutions of the complexes in acetonitrile. Electronic spectra in the UV-Vis range were recorded at 20ºC on a Perkin-Elmer Lambda 900 UV-Vis spectrophotometer using 1.0 cm quartz cells. Reflectance spectra were recorded on a Perkin-Elmer Lambda 900 spectrometer equipped with a biconical diffuse reflectance PELA-1022 accessory. Variable-temperature magnetic susceptibility measurements were carried out using microcrystalline samples (20–60 mg) of compounds **1** and **2**, using a Quantum Design MPMS2 SQUID susceptometer equipped with a 5.5 T magnet, operating at 0.1–0.5 T and at temperatures from 300–1.8 K. The susceptometer was calibrated with $(NH_4)_2Mn(SO_4)_2 \cdot 12H_2O$. Experimental susceptibilities were corrected for diamagnetism of the constituent atoms by the use of Pascal's constants.

X-Ray data collections and structure determinations

Crystal data, details on data collection and refinement are summarized in Table 1. Three-dimensional X-ray data were collected on a Bruker SMART 1000 CCD diffractometer by the ϕ–ω scan method. Reflections were measured from a hemisphere of data collected of frames each covering 0.3º in ω. Of the 7859 and

24618 reflections measured for complexes **1** and **2**, all of which were corrected for Lorentz and polarization effects and for absorption by multi-scan methods based on symmetry-equivalent and repeated reflections, 3558 and 5471 independent reflections exceeded the significance level $|F|/\sigma|F| > 4.0$, respectively. Complex scattering factors were taken from the program package SHELXTL[26] as implemented on a Pentium® computer. The structures were solved by direct methods and refined by full-matrix least-squares methods on F^2. The hydrogen atoms were included in calculated positions and refined by using a riding mode. Refinement converged with allowance for thermal anisotropy of all non-hydrogen atoms in all compounds. Minimum and maximum final electron density of −0.486 and 0.517 e Å^{-3} for **1** and −0.417 and 0.809 e Å^{-3} for **2** were found. The structure of **1** presents a slight disorder on an oxygen of one ionic perchlorate and the structure of **2** presents disorder in several ionic perchlorates. These disorders have been resolved and two atomic sites have been observed and refined with isotropic atomic displacement parameters in each case. The sites occupancy factors were 0.69(3) for O(4A) in **1** and 0.44(4) for O(12A), 0.68(6) for O(13A), 0.680(13) for O(17A), O(18A), O(19A) and O(20A), 0.553(18) for O(21A), O(22A), O(23A) and O(24A), 0.523(19) for O(26A) and O(28A) and 0.41(3) for O(29A) in **2**.

CCDC reference numbers 265325 (compound **1**) and 238131 (compound **2**).

See http://www.rsc.org/suppdata/dt/b5/b503151f/ for crystallographic data in CIF or other electronic format.

Table 1. Crystal data and structure refinement for **1** and **2**.

	1	**2**
Formula	$C_{38}H_{58}Cl_4N_{10}Ni_2O_{20}$	$C_{28}H_{44}Cl_3Co_2N_5O_{17}$
M_r	1234.12	946.89
Crystal system	Triclinic	Triclinic
Space group	$P\bar{1}$	$P\bar{1}$
T/K	293(2)	298(2)
a/Å	11.032(2)	12.839(2)
b/Å	11.376(3)	17.753(3)
c/Å	11.665(2)	18.532(3)
α/°	86.993(4)	84.699(4)
β/°	65.913(4)	71.771(3)
γ/°	81.707(4)	82.569(4)
V/Å^3	1322.5(5)	3972.3(12)
F(000)	640	1952
Z	1	4
D_c/g cm^{-3}	1.550	1.583
μ/mm^{-1}	0.996	1.113
R_{int}	0.0288	0.0319
Reflections measured	7859	24618
Reflections observed	3558	5471
Goodness-of-fit on F^2	1.008	0.891
R_1[a]	0.0584	0.0563
wR_2 (all data)[b]	0.1704	0.1907

[a] $R_1 = \Sigma||F_o| - |F_c||/\Sigma|F_o|$. [b] $wR_2 = \{\Sigma[w(||F_o|^2 - |F_c|^2|)^2]/\Sigma[w(F_o^4)]\}^{1/2}$.

Results and discussion

Synthesis and X-ray crystal structures

The reaction of the bibracchial lariat ether *N*,*N*′-Bis(2-aminobenzyl)-4,13-diaza-18-crown-6 (L) with nickel(II) perchlorate in acetonitrile solution gives the analytically pure product of formula $[Ni_2(L)(CH_3CN)_4](ClO_4)_4 \cdot CH_3CN$ (**1**). The molar conductivity Λ_M at 20 ºC in *ca.* 10^{-3} M acetonitrile solution is 455 $cm^2\ \Omega^{-1}\ mol^{-1}$, revealing that this compound behaves as a 4 : 1 electrolyte in this solvent.[27] The IR spectrum (KBr disks) shows bands due to the ν_{as}(Cl–O) stretching and δ_{as}(O– Cl–O) bending modes of the perchlorate groups[28] at *ca.* 1100 and 625 cm^{-1} without splitting, indicating uncoordinated anions, so suggesting that the perchlorate anions are not coordinated to the nickel ion in the solid state.

The solid-state structure of compound **1** was determined by single-crystal X-ray diffraction analysis, confirming the presence of two nickel(II) ions coordinated to the macrocyclic receptor. Compound **1** crystallizes in the $P\bar{1}$ triclinic space group. Crystals contain the binuclear centrosymmetric cation $[Ni_2(L)(CH_3CN)_4]^{4+}$ and well-separated perchlorate anions as well as acetonitrile molecules. Table 2 summarizes selected bond lengths and angles of the Ni(II) coordination environment, and the structure of the $[Ni_2(L)(CH_3CN)_4]^{4+}$ cation is depicted in Fig. 1. Each Ni(II) ion is bound to a pivotal nitrogen atom, one aniline nitrogen atom and to two oxygen atoms of the crown moiety. Coordination number six is completed by two nitrogen atoms of two solvent acetonitrile molecules. The amine nitrogen atoms N(1) and N(2), the nitrogen atom of an acetonitrile solvent molecule N(1S) and one oxygen atom of the crown moiety, O(1), are disposed meridionally, whereas the nitrogen atom of the second acetonitrile molecule, N(2S), and another oxygen atom of the crown moiety, O(2A), are axially coordinated. The coordination sphere around each Ni(II) ion can be described as a distorted octahedron, with the *trans* angles N(2S)–Ni(1)–O(2A) [178.23(12)º], N(1)–Ni(1)–O(1) [169.72(13)º] and N(2)–Ni(1)–N(1S) [173.05(13)º] close to linearity, as expected.

Table 2. Selected bond lengths (Å) and angles (º) for compound **1**[a]

Ni(1)–N(1S)	2.035(4)	Ni(1)–N(1)	2.098(4)
Ni(1)–N(2)	2.045(3)	Ni(1)–O(1)	2.117(3)
Ni(1)–N(2S)	2.095(4)	Ni(1)–O(2A)	2.150(3)
N(1S)–Ni(1)–N(2)	173.05(13)	N(2S)–Ni(1)–O(1)	85.61(13)
N(1S)–Ni(1)–N(2S)	87.90(15)	N(1)–Ni(1)–O(1)	169.72(13)
N(2)–Ni(1)–N(2S)	96.65(14)	N(1S)–Ni(1)–O(2A)	93.52(13)
N(1S)–Ni(1)–N(1)	91.77(15)	N(2)–Ni(1)–O(2A)	82.04(12)
N(2)–Ni(1)–N(1)	93.68(14)	N(2S)–Ni(1)–O(2A)	178.23(12)
N(2S)–Ni(1)–N(1)	87.37(15)	N(1)–Ni(1)–O(2A)	91.53(13)
N(1S)–Ni(1)–O(1)	95.47(13)	O(1)–Ni(1)–O(2A)	95.30(11)
N(2)–Ni(1)–O(1)	79.70(12)		

[a] Symmetry transformations used to generate equivalent atoms: A $-x + 1, -y + 1, -z + 2$.

Reaction of the bibracchial lariat ether L with cobalt(II) perchlorate in acetonitrile solution, under similar conditions as used for preparing compound **1**, gave the analytically pure product of formula $[Co(L)(\mu\text{-}OH)Co(CH_3CN)](ClO_4)_3$ (**2**). Its FAB-mass spectrum (Fig. 2) displays fragmentation peaks that confirm the

presence of two Co(II) ions coordinated to the receptor and the presence of a OH^- ligand, with the CH_3CN ligands being lost during the ionization process: $[Co_2(L)(\mu\text{-}OH)(ClO_4)_2]^+$ (*m*/*z* 805, 45% BPI), $[Co_2(L)(\mu\text{-}OH)(ClO_4)]^+$ (*m*/*z* 705, 12% BPI), $[Co_2(L)(ClO_4)_2]^+$ (*m*/*z* 787, 15% BPI), $[Co_2(L)(ClO_4)]^+$ (*m*/*z* 687, 29% BPI). The molar conductivity Λ_M at 20 ºC in *ca.* 10^{-3} M acetonitrile solution is 330 $cm^2\ \Omega^{-1}\ mol^{-1}$, revealing that this compound behaves as a 3 : 1 electrolyte in this solvent. The reaction of L with cobalt(II) to form the hydroxide-bridged binuclear Co(II) complex shows a high reproducibility since the cobalt bimetallic compound **2** can be systematically isolated from the reaction mixture in 45–55% yield. All of this points that under similar synthetic conditions very different products are obtained for nickel and cobalt. Martell and co-workers[29] found that certain macrocyclic binucleating ligands stabilise bridging of the two bound metal ions by hydroxo groups. They also found that while the binuclear Co(II) complex formed two hydroxo bridges the binuclear Ni(II) complex formed a single one, which suggests that some binuclear Co(II) complexes present a stronger affinity to form hydroxo bridges than the corresponding Ni(II) complexes. These results are in agreement with those reported in this work.

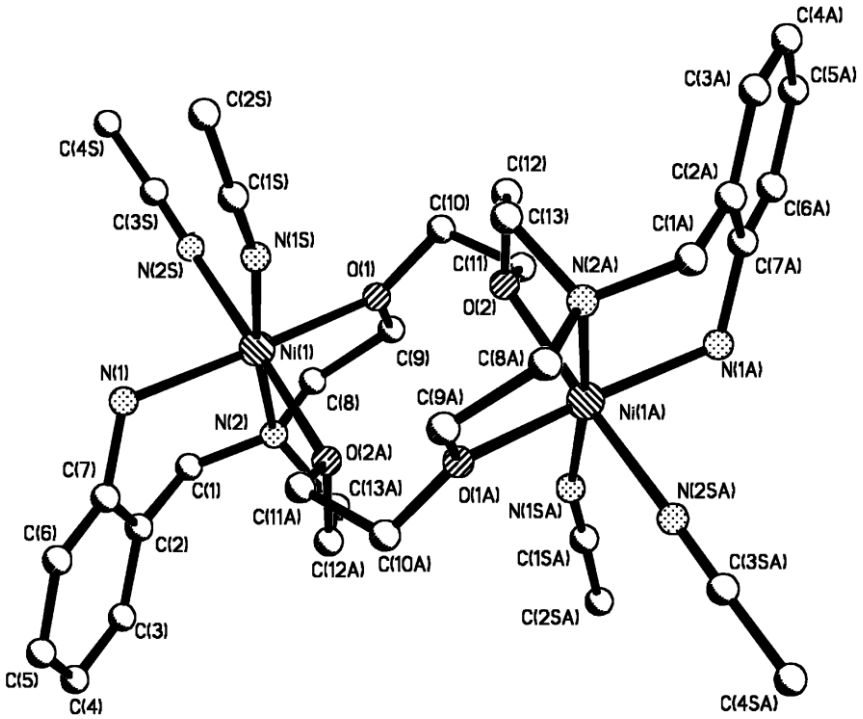

Fig. 1. Crystal structure of the $[Ni_2(L)(CH_3CN)_4]^{4+}$ cation in compound **1**. Hydrogen atoms are omitted for simplicity.

Compound **2** crystallizes in the triclinic space group $P\bar{1}$, and the asymmetric unit contains two different $[Co(L)(\mu\text{-}OH)Co(CH_3CN)](ClO_4)_3$ complex salts with slightly different bond distances and angles. Selected bond distances and angles are listed in Table 3, whereas the structures of the two $[Co(L)(\mu\text{-}OH)Co(CH_3CN)]^{3+}$ cations are depicted in Fig. 3. This figure clearly shows how the two cobalt(II) ions of the same binuclear cation display very different coordination environments. So, each of them is coordinated to two oxygen atoms of the crown moiety, one pivotal nitrogen atom, an amine nitrogen atom of the pendant arm, and a bridging hydroxo group. However, whereas one of the Co(II) ions is only five-coordinate, the other is six-coordinate where an acetonitrile molecule occupies the sixth coordination position. The five-coordinate Co(II) ion is found in a distorted trigonal-bipyramidal coordination environment, as indicated from the value of the index of trigonality τ[30] of 0.77 (τ = 0 for a perfectly square-pyramidal geometry and τ = 1 for a regular trigonal-bipyramidal geometry).[31] The six-coordinate Co(II) ion is found in a distorted octahedral arrangement where the amine nitrogen atoms N(1) and N(3), the oxygen atom of the hydroxo

group [O(1W)], and an oxygen atom of the crown moiety [O(1)] form the equatorial plane, while the apical positions are taken up by a nitrogen atom of an acetonitrile molecule [N(1S)] and an oxygen atom of the crown moiety [O(3)]. The *trans* angles N(1S)–Co(1)–O(3) [170.9(3)º] and N(1)–Co(1)–O(1W) [166.4(3)º] are close to linearity, while the third one O(1)–Co(1)–N(3) [160.0(3)º] is slightly off. The *cis* angles in the equatorial planes total *ca.* 360º, as expected. The intramolecular distance between the two Co(II) ions is 3.48 Å, while the Co–μ(OH)–Co angle amounts to *ca.* 128º.

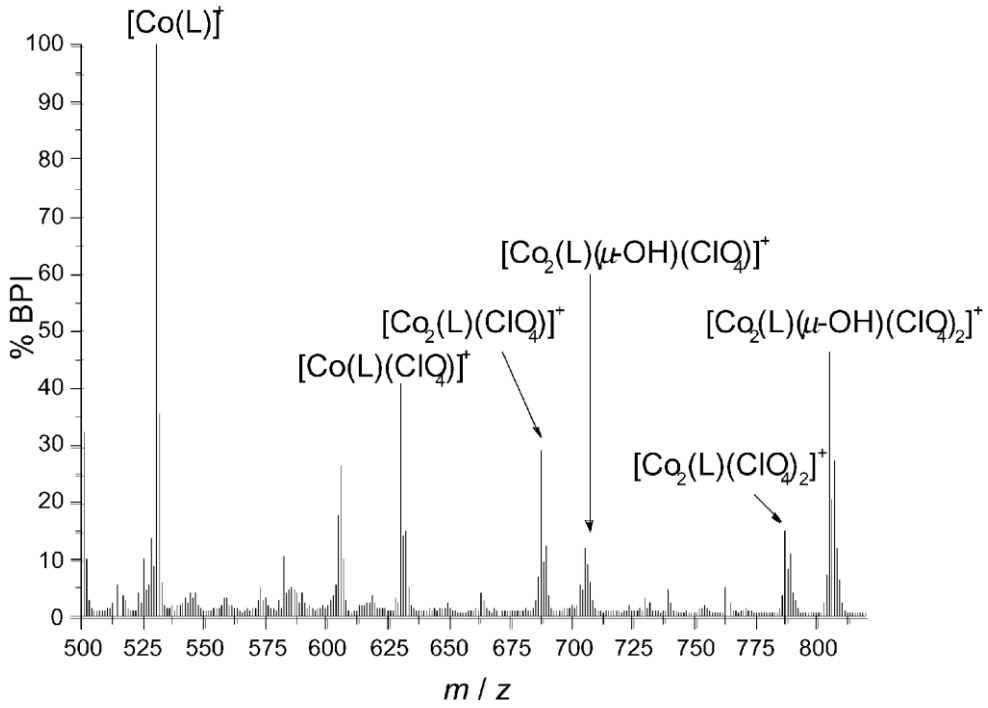

Fig. 2. Positive-ion FAB mass spectrum of compound **2**.

A classification of the potential coordination environments available to binuclear sites have been made:[32] (i) symmetric, (ii) donor asymmetry, (iii) geometric asymmetry and (iv) coordination number asymmetry. The binuclear core of compound **2** corresponds to (iv), in which an unequal number of donor atoms are coordinated to each metal atom, while the Ni(II) complex **1** presents a symmetric coordination environment. Several examples of bimetallic Co(II) complexes bearing fiveand six-coordinate sites[33,34] have been reported in the literature, although the use of unsymmetrical ligands have been always required to generate the two different coordination environments.[35] Compound **2** is the first example of a bimetallic Co(II) complex bearing five- and six-coordinate sites prepared by using a symmetrical polydentate ligand.

The flexibility of the lariat ether L allows this receptor to adopt both *syn* and *anti* conformations depending on factors such as the size and nature of the metal ion guest. In the case of compound **2**, the presence of a bridging hydroxo group together with the position of both Co(II) ions above the mean plane of the crown moiety forces the macrocyclic receptor to adopt a *syn* conformation. However, the bibracchial lariat ether L shows an *anti* arrangement in compound **1**, with both pendant arms disposed on opposite sides of the crown moiety. The presence of a hydroxo bridging ligand in **2** brings both Co(II) ions close together and so, whereas both Ni(II) ions are far apart (5.31 Å) in **1**, the distance between both Co(II) ions in **2** only amounts to 3.48 Å.

Table 3. Selected bond lengths (Å) and angles (º) for compound **2**.

Co(1)–O(1W)	1.946(6)	Co(3)–O(2W)	1.941(6)
Co(1)–N(1S)	2.132(8)	Co(3)–N(2S)	2.138(8)
Co(1)–N(1)	2.133(7)	Co(3)–N(5)	2.144(7)
Co(1)–N(3)	2.153(8)	Co(3)–N(7)	2.173(7)
Co(1)–O(1)	2.279(7)	Co(3)–O(5)	2.280(7)
Co(1)–O(3)	2.274(6)	Co(3)–O(7)	2.284(6)
Co(2)–O(2)	2.087(7)	Co(4)–O(6)	2.095(7)
Co(2)–O(1W)	1.933(6)	Co(4)–O(2W)	1.928(6)
Co(2)–N(2)	2.177(9)	Co(4)–N(6)	2.165(9)
Co(2)–O(4)	2.069(6)	Co(4)–O(8)	2.082(6)
Co(2)–N(4)	2.079(8)	Co(4)–N(8)	2.078(8)
O(1W)–Co(1)–N(1S)	93.1(3)	O(2W)–Co(3)–N(2S)	92.8(3)
O(1W)–Co(1)–N(1)	166.4(3)	O(2W)–Co(3)–N(5)	165.9(3)
N(1S)–Co(1)–N(1)	99.7(3)	N(2S)–Co(3)–N(5)	100.2(3)
O(1W)–Co(1)–N(3)	95.7(3)	O(2W)–Co(3)–N(7)	96.0(3)
N(1S)–Co(1)–N(3)	85.1(3)	N(2S)–Co(3)–N(7)	85.8(3)
N(1)–Co(1)–N(3)	89.9(3)	N(5)–Co(3)–N(7)	90.2(3)
O(1W)–Co(1)–O(3)	87.1(2)	O(2W)–Co(3)–O(7)	86.7(2)
N(1S)–Co(1)–O(3)	170.9(3)	N(2S)–Co(3)–O(7)	170.8(3)
N(1)–Co(1)–O(3)	79.5(3)	N(5)–Co(3)–O(7)	79.5(3)
N(3)–Co(1)–O(3)	103.9(3)	N(7)–Co(3)–O(7)	103.4(3)
O(1W)–Co(1)–O(1)	100.8(3)	O(2W)–Co(3)–O(5)	99.7(3)
N(1S)–Co(1)–O(1)	82.8(3)	N(2S)–Co(3)–O(5)	83.5(3)
N(1)–Co(1)–O(1)	76.6(3)	N(5)–Co(3)–O(5)	76.8(3)
N(3)–Co(1)–O(1)	160.0(3)	N(7)–Co(3)–O(5)	161.4(3)
O(3)–Co(1)–O(1)	88.3(2)	O(7)–Co(3)–O(5)	87.5(2)
O(1W)–Co(2)–O(4)	100.8(3)	O(2W)–Co(4)–O(8)	100.2(3)
O(1W)–Co(2)–N(4)	98.2(3)	O(2W)–Co(4)–N(8)	97.4(3)
O(4)–Co(2)–N(4)	118.8(3)	O(8)–Co(4)–N(8)	119.4(3)
O(1W)–Co(2)–O(2)	94.2(3)	O(2W)–Co(4)–O(6)	93.6(3)
O(4)–Co(2)–O(2)	124.3(3)	O(8)–Co(4)–O(6)	125.2(3)
N(4)–Co(2)–O(2)	111.4(4)	N(8)–Co(4)–O(6)	110.7(4)
O(1W)–Co(2)–N(2)	172.0(3)	O(2W)–Co(4)–N(6)	170.9(3)
O(4)–Co(2)–N(2)	77.9(3)	O(8)–Co(4)–N(6)	79.4(3)
N(4)–Co(2)–N(2)	89.3(3)	N(8)–Co(4)–N(6)	90.6(3)
O(2)–Co(2)–N(2)	80.3(3)	O(6)–Co(4)–N(6)	79.4(3)

Recent structural determinations of human methionine aminopeptidase (MAP) and MAP from *Pyrococcus furious* revealed structurally analogous bicobalt(II) centers in the active sites. They consist of two metal ions bridged by either a water molecule or a hydroxide ion, and coordinated to two aspartames, two glutamates and one histidine residue.[36] A recent determination of the structure of MAP from *Escherichia coli* has revealed the presence of two Co(II) ions with different coordination numbers (Fig. 4):[37] one of the Co(II) ions is hexacoordinated in a distorted octahedral environment (with a coordinated water molecule completing the coordination number six), whereas the second Co(II) ion is pentacoordinated in a distorted trigonal-bipyramidal arrangement; a hydroxide group acts as a bridge between both Co(II) ions.[37] The index of

trigonality τ for the pentacoordinated Co(II) ion in MAP from *Escherichia coli* amounts to 0.83 (τ = 0.77 for **2**). The distance between the two Co(II) ions amounts to 3.16 Å, only *ca.* 0.3 Å shorter than that found in **2**. Thus, the solid-state structure of compound **2** presents features that structurally resemble the active site of MAP from *Escherichia coli*.

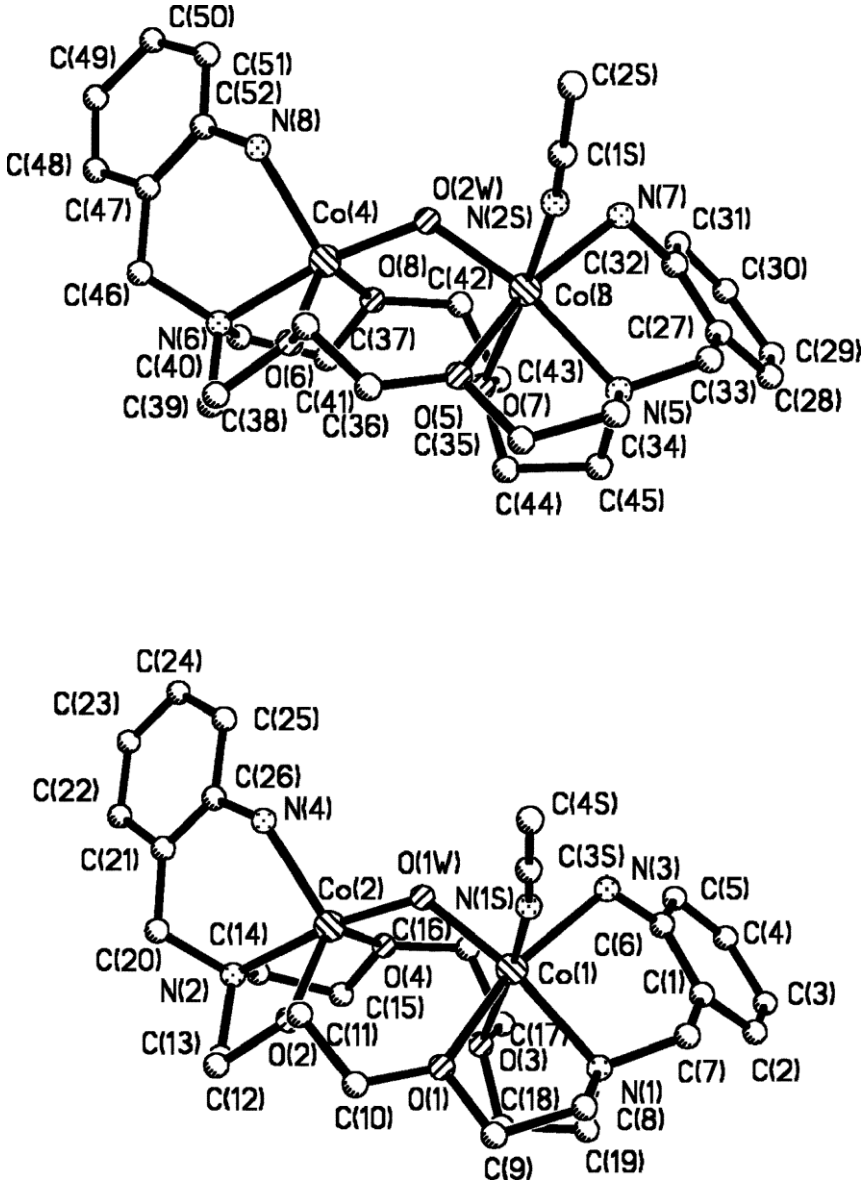

Fig. 3. Crystal structures of the $[Co_2(L)(\mu\text{-}OH)(CH_3CN)]^{3+}$ cations in compound **2**. Hydrogen atoms are omitted for simplicity

Magnetic properties

The magnetic behavior of **1** is shown in Fig. 5 as the $\chi_M T$ product *vs.* T where χ_M is the molar magnetic susceptibility and T the temperature. The $\chi_M T$ product is *ca.* 2.51 cm^3 K mol^{-1} at 300 K and remains constant down to 50 K. This value is typical for two uncoupled S = 1 spins. $\chi_M T$ decreases significantly at lower temperatures to attain a value of 1.44 cm^3 K mol^{-1} at 2.0 K. Intramolecular magnetic exchange has been ruled out as the pathway O(1)–C(10)–C(11)–O(2) connecting the two Ni(II) centres is too long and inefficient to afford significant overlapping between the orbitals containing the unpaired electrons.

Consequently, the low-temperature behaviour reflects essentially the occurrence of zero-field splitting of the S = 1 ground state of the nickel(II) centres. Hence we have analyzed the $\chi_M T$ *vs.* T data using the Hamiltonian:

$$\hat{H} = D\left[\hat{S}_z^2 - (1/3)S(S+1)\right] + g\beta H\hat{S} \qquad (1)$$

where D corresponds to the zero-field splitting parameter.[10] The best fit for calculated and experimental $\chi_M T$ values has been found for D = 6 cm^{-1}, g = 2.24 and R = 2.5 × 10^{-4}; R is the agreement factor defined as $\Sigma_i[(\chi_M)_i^{exptl} - (\chi_M)_i^{calc}]^2/\Sigma_i[(\chi_M)_i^{exptl}]^2$. The solid line in Fig. 5 corresponds to the calculated curve showing that an excellent agreement between the experimental and theoretical $\chi_M T$ data is achieved. The obtained D value is within the normal limits observed for pseudo-octahedral Ni(II) complexes.

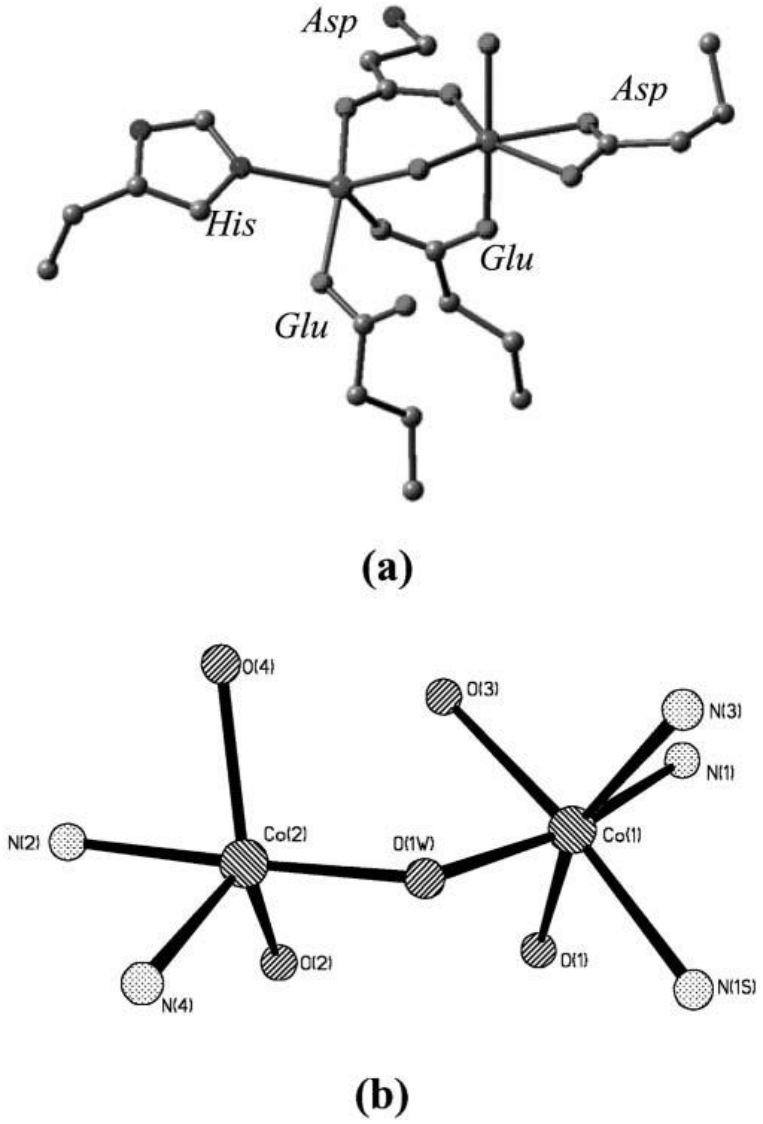

Fig. 4. (a) Structure of the catalytic bimetallic core of the *Escherichia coli* methionine aminopeptidase. Coordinates are from the Brookhaven Databank (PDB code 2MAT). (b) View of the bimetallic core in compound **2**.

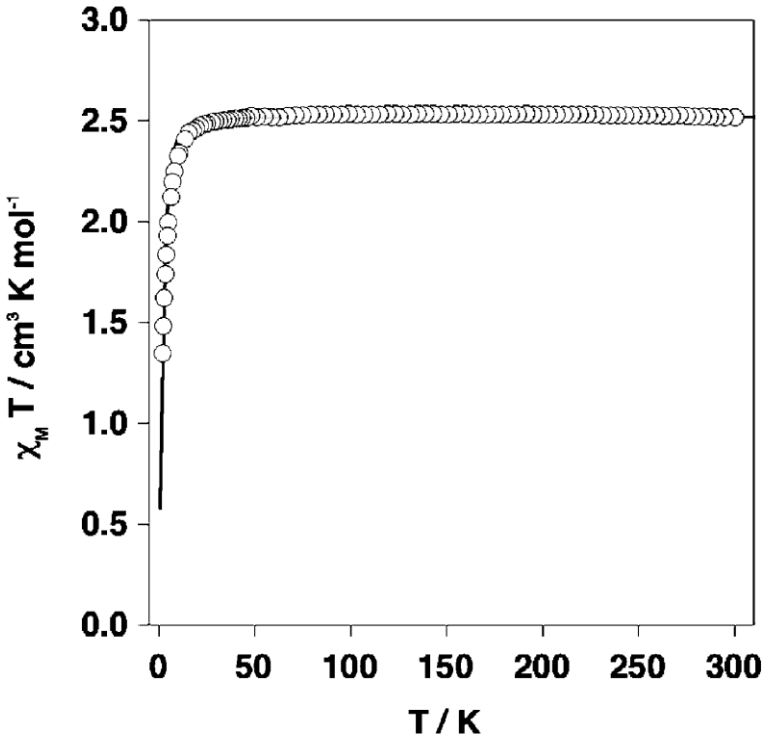

Fig. 5. Temperature dependence of the $\chi_M T$ product for compound **1**. The solid line represents the best fit of the experimental data as discussed in the text.

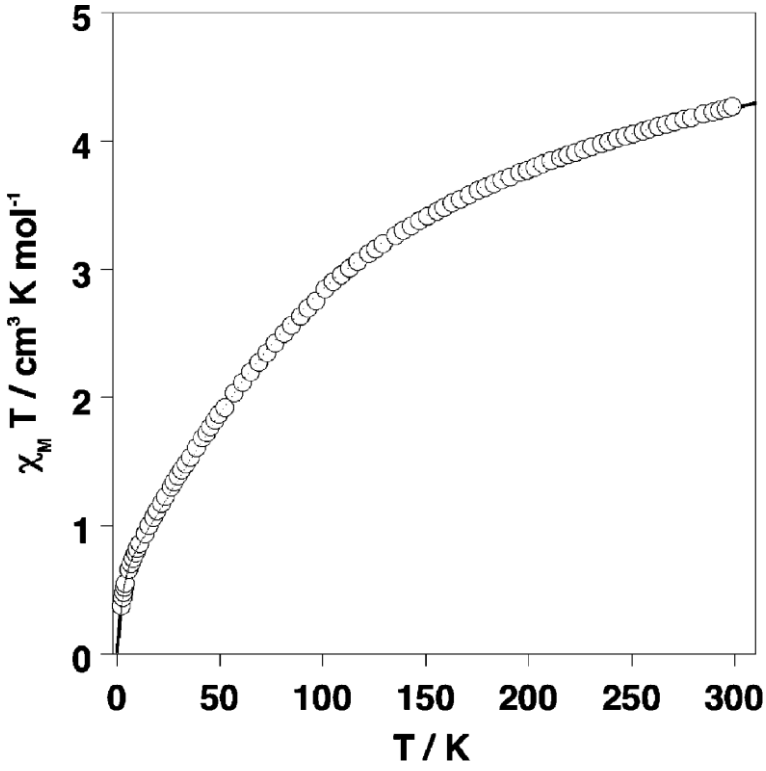

Fig. 6. Temperature dependence of the $\chi_M T$ product for compound **2**. The solid line represents the best fit of the experimental data as discussed in the text.

The $\chi_M T$ *vs. T* curve for **2** is displayed in Fig. 6. At 300 K the $\chi_M T$ is 4.26 cm^3 K mol^{-1}, a reasonable value for two Co(II) ions in which an important orbital contribution is involved. $\chi_M T$ continuously decreases with temperature to a value of 0.37 cm^3 K mol^{-1} at 2 K. This behaviour indicates the occurrence of intramolecular antiferromagnetic coupling mediated by the OH^- bridge. However, the χ_M *vs. T* curve does not display the expected maximum. Any attempt to fit these data using the HDVV Hamiltonian describing the isotropic interaction, *J*, between two identical $S = 3/2$ centres or considering spin– orbit coupling in the dimer as described by Lines' theory,[38] was unsuccessful. This is probably due to the asymmetric nature of the binuclear system.

In order to evaluate the exchange coupling constant, *J*, for **2** we have assumed that the ground state of the six-coordinate Co(II) ion $^4T_1$ ($S_1 = 3/2$ and fictitious angular momentum $L_1 = 1$) splits into a sextet, a quartet, and a Kramers doublet by spin–orbit coupling. The corresponding Hamiltonian is:

$$\hat{H}_{SO} = Ak\lambda\hat{L}_1\hat{S}_1 \qquad (2)$$

where *k* is the orbital reduction factor and λ is the spin–orbit coupling constant. The *A* factor is defined in the context of T and P term isomorphism and enables us to distinguish between the matrix elements of the orbital angular momentum operator calculated with the wave functions of the $^4T_1$ term with those calculated with the use of the P term basis.[10,39] We have also considered the effect of an axial distortion. Under an axial distortion, the triplet orbital $^4T_1$ ground state splits into a singlet $^4A_2$ and a doublet ^4E levels with an energy gap Δ. The corresponding operator is given in eqn. (3):

$$M_{ax} = \Delta\left[\hat{L}_{1z}{}^2 - (1/3)L_1(L_1+1)\right] \qquad (3)$$

As far as the five-coordinated Co(II) ion is concerned, we assume that first order spin–orbit coupling is completely quenched and that the resulting orbital singlet ground state ($S_2 = 3/2$) splits due to zero-field splitting (see eq 1) being 2D the energy gap between the $M_S = 3/2$ and 1/2 levels.

The complete Hamiltonian which describes the system can be written

$$\hat{H} = 2J\hat{S}_1\hat{S}_2 + AK\lambda\hat{S}_1\hat{L}_1 + \Delta\left[\hat{L}_{1z}{}^2 - (1/3)L_1(L_1+1)\right] + D\left[\hat{S}_{2z}{}^2 - (1/3)S_2(S_2+1)\right] \qquad (4)$$

where the first term involves the exchange interaction between Co(II) ions, whereas the second represents the spin– orbit coupling in an octahedral Co(II) ion. The third term corresponds to low-symmetry (noncubic) crystal field term for the octahedral Co(II) ion and the fourth term is the zero-field splitting associated to the second Co(II) ion. Finally, the Zeeman interaction is assumed to be isotropic and can be presented as

$$\hat{H}_{Zee} = \beta\left(g_e\hat{S}_1 + Ak\hat{L}_1\right)H + \beta g_2\hat{S}_2 H \qquad (5)$$

The first term describes the interaction of an octahedral Co(II) ion with an external magnetic field including both spin and orbital Zeeman contributions (g_e is the electronic *g*-factor) and the second term only considers the spin Zeeman contribution of the pentacoordinate Co(II) (g_2 is the *g* factor for the Co(II) ion).

No analytical expression for the magnetic susceptibility as a function of *A*, *k*, λ, *J* and *D* can be derived. The values of these parameters were derived using an exact diagonalization process.[40,41] The best fit between calculated and experimental data corresponds to $\lambda = -100.5$ cm^{-1}, $k = 0.90$ (fixed), $A = -1$ (fixed), $D = -780$ cm^{-1}, $J = -13.1$ cm^{-1}, $D = 17.3$ cm^{-1}, $g_2 = 2.10$, TIP = 1.8×10^{-3} (TIP corresponds to the temperature independent paramagnetism parameter) and $R = 2 \times 10^{-4}$. No other minima were found in the fit-procedure. The calculated curve and experimental data match very well in the whole range of temperatures (Fig. 6). The spin–orbit coupling parameter is smaller than that considered for the free Co(II) ion, −160 cm^{-1}, but is close to that obtained for other binuclear Co(II) complexes.[42] The negative value of parameter Δ means that the doublet $^4E_2$ state is the fundamental and lies below the $^4A_2$ state by *ca.* 780 cm^{-1}, a value which is reasonable for the coordination geometry of six-coordinate Co(II) ions. The *D* value obtained for singlet orbital ground state of the five-coordinate Co(II) is also within the normal limits observed for this ion. Finally, the exchange coupling between degenerated and not degenerated orbital Co(II) ions is antiferromagnetic and similar to previous examples.[43] D'Souza *et al.*[44] reported a ferromagnetic interaction between the two Co(II) ions of MAP from *Escherichia coli* on the basis of EPR measurements at pH = 9.5. The different magnetic behaviour of compound **2** and its biological counterpart is most probably due to the fact that the Co(1)–O(1W)–Co(2) angle is more open in **2** (127.9º) than in the protein (97.5º). The use of additional bridging ligands could allow a modulation of this angle and therefore a fine control of the magnetic properties in this class of compounds.

Conclusions

Unlike with the related *N*,*N*′-bis(2-aminobenzyl)-1,10-diaza-15-crown-5 that, with the first-row transition metal ions: Mn(II), Co(II), Ni(II), Cu(II) and Zn(II), only forms mononuclear complexes and dominates over the coordinative preferences of the particular cation guests, *N*,*N*′-bis(2-aminobenzyl)-4,13- diaza-18-crown-6 (L) is a versatile receptor able to adapt to the coordinative preferences of different metal cation guests. Herein we have shown that L is able to form binuclear complexes with both Ni(II) and Co(II) ions. However, the structure of both complexes is quite different. The X-ray structure of the symmetrical Ni(II) complex shows an *anti* arrangement of the two pendants of the ligand, and both Ni(II) ions are sixcoordinate in distorted octahedral environments. With Co(II), L forms a hydroxo-bridged binuclear complex showing structural features that structurally mimic the active site of methionine aminopeptidases and containing two Co(II) ions with different coordination environments. Likewise, the presence of a hydroxo bridging group in the unusual Co(II) complex allows the presence of antiferromagnetic exchange in this compound. This magnetic behaviour has been satisfactorily analyzed considering firstorder spin–orbit coupling in the assumed axially distorted octahedral site and totally quenched orbital contribution in the five-coordinate site in which zero-field splitting of the $S = 3/2$ ground state is operative.

Acknowledgments

L.V, C. P.-I., D. E.-G, F. A. A. de B. and T. R.-B. thank Xunta de Galicia (PGIDIT03TAM10301PR) for generous financial support. J. M. C.-J. and J. A. R. are grateful for financial support from the Spanish DGICYT through Project CTQ 2004-03456.

References

1. J. A. Real, A. B. Gaspar, M. C. Muñoz, P. Gütlich, V. Ksenofontov and H. Spiering, *Top. Curr. Chem*., 2004, **233**, 167.

2. E. Breuning, M. Ruben, J.-M. Lehn, F. Renz, Y. Garcia, V. Ksenofontov, P. Gütlich, E. Wegelius and K. Rissanen, *Angew. Chem., Int. Ed*., 2000, **39**, 2504.

3. G. M. Ferrence, E. Simón-Manso, B. K. Breedlove, L. Meeuwenberg and C. P. Kubiak, *Inorg. Chem.*, 2004, **43**, 1071.

4. E. I. Solomon, T. C. Brunold, M. I. Davis, J. N. Kemsley, S.-K. Lee, N. Lehnert, F. Neese, A. J. Skulan, Y.-S. Yang and J. Zhou, *Chem. Rev*., 2000, **100**, 235.

5. M. Kobayashi and S. Shimizu, *Eur. J. Biochem*., 1999, **261**, 1.

6. R. P. Hausinger, *Biochemistry of Nickel*, Plenum Press, New York, 1993.

7. D. E. Wilcox, *Chem. Rev*., 1996, **96**, 2435.

8. E. Jabri, M. B. Carr, R. P. Hausinger and P. A. Karplus, *Science*, 1995, **268**, 998.

9. S. L. Roderick and B. W. Matthews, *Biochemistry*, 1993, **32**, 3907.

10. O. Kahn, *Molecular Magnetism*, VCH, New York, 1993.

11. D. A. Brown, W. Errington, W. K. Glass, W. Haase, T. J. Kemp, H. Nimir, S. M. Ostrovsky and R. Werner, *Inorg. Chem*., 2001, **40**, 5962.

12. C. Incarvito, A. L. Rheingold, C. J. Qin, A. L. Gavrilova and B. Bosnich, *Inorg. Chem*., 2001, **40**, 1386.

13. G. Dong, P. Ke-liang, D. Chun-ying, H. Cheng and M. Qing-jin, *Inorg. Chem*., 2002, **41**, 5978.

14. A. L. Gavrilova, C.-J. Qin, R. D. Sommer, A. L. Rheingold and B. Bosnich, *J. Am. Chem. Soc*., 2002, **124**, 1714.

15. D. Ghosh, S. Mukhopadhyay, S. Samanta, K.-Y. Choi, A. Endo and M. Chaudhury, *Inorg. Chem*., 2003, **42**, 7189.

16. B. Kersting, *Angew. Chem., Int. Ed*., 2001, **40**, 3988.

17. E. Vogel, M. Michels, L. Zander, J. Lex, N. S. Tuzun and K. N. Houk, *Angew. Chem., Int. Ed*., 2003, **42**, 2857.

18. A. E. Martell, R. J. Motekaitis, D. Chen and R. E. Hancock, *Supramol. Chem*., 1996, **6**, 333.

19. D. S. Cati, J. Ribas, J. Ribas-Ariño and H. Stoeckli-Evans, *Inorg. Chem*., 2004, **43**, 1021.

20. D. Esteban, D. Bañobre, R. Bastida, A. de Blas, A. Macías, A. Rodríguez, T. Rodríguez-Blas, D. E. Fenton, H. Adams and J. Mahía, *Inorg. Chem*., 1999, **38**, 1937.

21. C. Platas-Iglesias, D. Esteban, V. Ojea, F. Avecilla, A. de Blas and T. Rodríguez-Blas, *Inorg. Chem*., 2003, **42**, 4299.

22. D. Esteban, D. Bañobre, A. de Blas, T. Rodríguez-Blas, R. Bastida, A. Macías, A. Rodríguez, D. E. Fenton, H. Adams and J. Mahía, *Eur. J. Inorg. Chem*., 2000, 1445.

23. D. Esteban, F. Avecilla, C. Platas-Iglesias, J. Mahía, A. de Blas and T. Rodríguez-Blas, *Inorg. Chem*., 2002, **41**, 4337.

24. C. Rodríguez-Infante, D. Esteban, F. Avecilla, A. de Blas, T. Rodríguez-Blas, J. Mahía, A. L. Macedo and C. F. G. C. Geraldes, *Inorg. Chim. Acta*, 2001, **317**, 190.

25. W. C. Wolsey, *J. Chem. Educ*., 1973, **50**, A335.

26. G. M. Sheldrick, *SHELXTL Bruker Analytical X-ray System, Release 5.1*, Madison, WI, 1997.

27. W. J. Geary, *Coord. Chem. Rev*., 1971, **7**, 81.

28. K. Nakamoto, *Infrared and Raman Spectra of Inorganic and Coordination Compounds*, J. Wiley, New York, Chichester, Brisbane and Toronto, 3rd edn., 1972, pp. 142–154.

29. R. J. Motekaitis, A. E. Martell, J.-M. Lehn and E.-I. Watanabe, *Inorg. Chem*., 1982, **21**, 4253.

30. The parameter τ is the index of the degree of trigonality within the structural continuum between square-pyramidal and trigonal-bipyramidal geometries. If A is the apical donor atom of a square-based pyramid then it should not be amongst the atoms which define the largest two angles at the metal center. Donor atoms B and C are associated with the greater basal angle (β) and atoms D and E with the smaller basal angle (a); $\tau = (\beta - a)/60$ and is therefore 0 for a square pyramid and 1 for a trigonal bipyramid.

31. W. Addison, T. Nageswara-Rao, J. Reedijk, J. van Rijn and G. C. Verschoor, *J. Chem. Soc., Dalton Trans*., 1984, 1349.

32. J. H. Satcher, Jr., M. W. Droege, T. J. R. Weakley and R. T. Taylor, *Inorg. Chem*., 1995, **34**, 3317.

33. A. L. Gavrilova, C.-J. Qin, R. D. Sommer, A. L. Rheingold and B. Bosnich, *J. Am. Chem. Soc*., 2002, **124**, 1219.

34. B. Incarvito, A. L. Rheingold, A. L. Gavrilova, C.-J. Qin and B. Bosnich, *Inorg. Chem*., 2001, **40**, 4101.

35. C. E. Fenton and H. Okawa, *Chem. Ber./Recueil*, 1997, **130**, 433.

36. W. T. Lowther and B. W. Matthews, *Chem. Rev*., 2002, **102**, 4581.

37. W. T. Lowther, A. M. Orville, D. T. Madden, S. Lim, D. H. Rich and B. W. Mattews, *Biochemistry*, 1999, **38**, 7678.

38. M. E. Lines, *J. Chem. Phys*., 1971, **55**, 2977.

39. F. E. Mabbs and D. J. Machin, *Magnetism and Transition Metal Complexes*, Chapman and Hall, London, 1973.

40. J. J. Borrás-Almenar, J. M. Clemente-Juan, E. Coronado and B. S. Tsukerblat, *Inorg. Chem*., 1999, **38**, 6081.

41. J. J. Borrás-Almenar, J. M. Clemente-Juan, E. Coronado and B. S. Tsukerblat, *J. Comput. Chem*., 2001, **22**, 985.

42. G. De Munno, M. Julve, F. Lloret, J. Faus and A. Caneschi, *J. Chem. Soc., Dalton Trans*., 1994, 1175.

43. H. Andres, M. Aebersold, H. U. Güdel, J. M. Clemente, E. Coronado, H. Büttner, D. Kearley and M. Zolliker, *Chem. Phys. Lett*., 1998, **289**, 224.

44. V. M. D'Souza, B. Bennett, A. J. Copik and R. C. Holz, *Biochemistry*, 2000, **39**, 3817.